J Neurophysiol 108: 714–728, 2012.
First published May 16, 2012; doi:10.1152/jn.00269.2012.

Neural ITD coding with bilateral cochlear implants: effect of binaurally coherent jitter

Kenneth E. Hancock,[1,2] Yoojin Chung,[1,2] and Bertrand Delgutte[1,2,3]

[1]*Eaton-Peabody Laboratories, Massachusetts Eye and Ear Infirmary, Boston, Massachusetts;* [2]*Department of Otology and Laryngology, Harvard Medical School, Boston, Massachusetts; and* [3]*Research Laboratory of Electronics, Massachusetts Institute of Technology, Cambridge, Massachusetts*

Submitted 30 March 2012; accepted in final form 10 May 2012

Hancock KE, Chung Y, Delgutte B. Neural ITD coding with bilateral cochlear implants: effect of binaurally coherent jitter. *J Neurophysiol* 108: 714–728, 2012. First published May 16, 2012; doi:10.1152/jn.00269.2012.—Poor sensitivity to the interaural time difference (ITD) constrains the ability of human bilateral cochlear implant users to listen in everyday noisy acoustic environments. ITD sensitivity to periodic pulse trains degrades sharply with increasing pulse rate but can be restored at high pulse rates by jittering the interpulse intervals in a binaurally coherent manner (Laback and Majdak. Binaural jitter improves interaural time-difference sensitivity of cochlear implantees at high pulse rates. *Proc Natl Acad Sci USA* 105: 814–817, 2008). We investigated the neural basis of the jitter effect by recording from single inferior colliculus (IC) neurons in bilaterally implanted, anesthetized cats. Neural responses to trains of biphasic pulses were measured as a function of pulse rate, jitter, and ITD. An effect of jitter on neural responses was most prominent for pulse rates above 300 pulses/s. High-rate periodic trains evoked only an onset response in most IC neurons, but introducing jitter increased ongoing firing rates in about half of these neurons. Neurons that had sustained responses to jittered high-rate pulse trains showed ITD tuning comparable with that produced by low-rate periodic pulse trains. Thus, jitter appears to improve neural ITD sensitivity by restoring sustained firing in many IC neurons. The effect of jitter on IC responses is qualitatively consistent with human psychophysics. Action potentials tended to occur reproducibly at sparse, preferred times across repeated presentations of high-rate jittered pulse trains. Spike triggered averaging of responses to jittered pulse trains revealed that firing was triggered by very short interpulse intervals. This suggests it may be possible to restore ITD sensitivity to periodic carriers by simply inserting short interpulse intervals at select times.

binaural hearing; temporal coding; congenital deafness; inferior colliculus; interaural time difference

INCREASING NUMBERS of deaf patients are receiving bilateral cochlear implants (CIs) with the goal of restoring the benefits of binaural hearing in everyday listening situations. Bilateral CIs do improve sound localization ability, but, in contrast to normal-hearing listeners, CI users are largely unable to use interaural time difference (ITD) cues, relying instead almost entirely on interaural level differences for sound localization (Aronoff et al. 2010; Seeber and Fastl 2008; van Hoesel 2004). Similarly, bilateral CIs improve speech understanding in noise, but mostly in circumstances when acoustical shadowing of the masking source by the head creates a favorable signal-to-noise ratio in one ear (Litovsky et al. 2006; Schleich et al. 2004; van Hoesel and Tyler 2003). Bilateral CI users show little or no binaural unmasking or "squelch," which results from central comparison of the inputs to the two ears and is important for listening in environments with spatially distributed maskers, such as multiple talkers or reverberation (Bronkhorst and Plomp 1992; Peissig and Kollmeier 1997; van Hoesel 2011; Zurek 1992).

Deficient ITD processing appears to limit binaural unmasking and sound localization by bilateral CI users. In particular, for constant-amplitude pulse trains, ITD discrimination thresholds degrade sharply for pulse rates above ~100 pulses/s (pps) (Laback et al. 2007; Poon et al. 2009; van Hoesel and Tyler 2003). Laback and Majdak (2008) proposed that degraded ITD discrimination at high pulse rates was a manifestation of "binaural adaptation," a dominance of onset cues in the lateralization of high-rate pulsatile stimuli (Buell and Hafter 1988). They hypothesized that continuously jittering (i.e., randomizing) the interpulse intervals with the CI would continuously restart the adaptation process (Hafter and Buell 1990) and thereby produce robust ITD sensitivity. Their psychophysical data showed that CI users indeed maintain good ITD discrimination as the pulse rate increases from 400 to 1,515 pps for jittered, but not periodic, pulse trains.

While it is clear that pulse train jitter improves ITD discrimination, debate persists regarding the underlying mechanism and the relationship to other binaural adaptation phenomena. There is particular disagreement about the relative importance of long and short interpulse intervals in mediating the jitter effect (Brown and Stecker 2011; Goupell et al. 2009; van Hoesel 2008a, 2008b).

We hypothesized that neurons in inferior colliculus (IC) show correlates of the jitter effect. As in psychophysical performance, the ITD sensitivity of most IC neurons in bilaterally implanted animals degrades at high pulse rates, where neurons only give an onset response to periodic pulse trains (Middlebrooks and Snyder 2010; Shepherd et al. 1999; Smith and Delgutte 2007a; Snyder et al. 1995). We characterized the ITD sensitivity of IC neurons for both periodic and jittered pulse trains in bilaterally implanted, anesthetized cats. The results were qualitatively consistent with the effect of jitter on ITD discrimination in human CI subjects. We found that jitter restores ongoing firing to high pulse rates in about half of IC neurons and, in so doing, reveals latent neural ITD sensitivity. Our analysis sheds light on the underlying mechanism by demonstrating that neural responses to jittered stimuli are triggered by short interpulse intervals.

Address for reprint requests and other correspondence: K. E. Hancock, Eaton-Peabody Laboratories, Massachusetts Eye and Ear Infirmary, Boston, MA 02114 (e-mail: Ken_Hancock@meei.harvard.edu).

METHODS

Experiments were performed on 15 anesthetized adult cats of either sex, who received bilateral cochlear implants at the time of experimentation. The cats comprised three groups differing in onset age and duration of deafness before implantation: acutely deafened cats (deaf for 1 wk, $n = 5$); long-term, adult-deafened cats (deaf for 6 mo, $n = 3$); and congenitally deaf white cats (deaf from birth, $n = 7$, age at time of experiment: 6–18 mo, mean: 10 mo). These groups model the variability in normal hearing experience across human CI users. The congenitally deaf and acutely deafened cats were also used in a previous study (Hancock et al. 2010) showing that ITD-sensitive IC neurons are about half as common in congenitally deaf cats compared with acutely deafened cats. All procedures were approved by the Animal Care Committees of the Massachusetts Eye and Ear Infirmary and Massachusetts Institute of Technology.

Deafening procedures. Cats in the acutely deafened and long-term deafened groups were anesthetized with ketamine (33 mg/kg im) and then deafened by the coadministration of kanamycin (300 mg/kg sc) and ethacrynic acid (25 mg/kg iv) (Xu et al. 1993). Long-term deafened cats were again anesthetized with ketamine 1 wk after being deafened, and deafness was verified by the absence of click-evoked auditory brain stem responses (ABRs) for intensities up to 100 dB sound pressure level (see Hancock et al. 2010 for ABR methods). Deafness in acutely deafened cats was verified using ABRs at the time of experimentation, ~1 wk after they were deafened.

There is significant variation among white cats with respect to cochlear pathology and degree of deafness (Ryugo et al. 1998, 2003). Therefore, deafness in this group was confirmed in the laboratory of Dr. David Ryugo (Johns Hopkins University) at 4 and 8 postnatal weeks using tone- and click-evoked ABR measurements (Ryugo et al. 2003).

Surgery and cochlear implantation. For electrophysiological recordings, all surgical and experimental procedures were performed under barbiturate anesthesia, either single injections of Dial-in-urethane (75 mg/kg ip diallylbarbituric acid + 300 mg/kg ip urethane) or separate injections of Nembutal (37 mg/kg ip) and urethane (300 mg/kg ip). Supplemental doses (~10% of the initial dose) were given as needed to maintain areflexia to strong toe pinches. Dexamethasone (0.2 ml im) was given every 4 h to minimize brain swelling, and the trachea was cannulated to maintain airway patency. Body temperature was maintained at 37°C using a feedback-controlled heating blanket. Heart rate, respiration rate, and expired CO_2 were monitored continuously throughout the experiment.

The lateral and dorsal aspects of the skull were exposed by reflecting the overlying tissue, and the pinnae were transected to facilitate placement of closed acoustic systems for measuring acoustic ABRs. On each side, the tympanic bulla was opened, and a CI with eight ring-type contacts (Cochlear) was inserted through a cochleostomy near the round window. An opening was made in the skull, and the dorsal surface of the IC was then exposed by aspirating the overlying occipital cortex and removing a portion of the bony tentorium.

Stimuli. Stimuli were 300-ms biphasic pulse trains (50-μs/phase, cathodic leading) presented every 600 ms. Stimuli were digitally synthesized using a sampling rate of 100 kHz. Jittered pulse trains (Fig. 1) were created following the method of Laback and Majdak (2008) with one difference. The previous study minimized onset ITD cues by applying 20-ms linear ramps to the pulse trains, whereas we did not impose a ramp but simply discarded the first 15 ms after the stimulus onset from the neural responses. For each pulse rate, interpulse intervals were randomly drawn from a rectangular distribution spanning ±90% of the mean interval (equal to 1/mean pulse rate). For example, a 640-pps pulse train (mean interval: 1.56 ms) with 90% jitter contains interpulse intervals between 0.156 and 2.97 ms. In some cases, the jitter was varied systematically from 10% to 90%. In the 640-pps example, a stimulus with 10% jitter contains intervals between 1.41 and 1.72 ms. In this report, "jittered pulse train" refers to 90% jitter unless otherwise noted. The jitter was binaurally coherent (same pulse sequence presented to each ear) to preserve fine-structure ITD. The jitter was "frozen" so that for each mean pulse rate, the identical sequence of pulses was presented on every repetition. The same pulse sequence was used for all neurons and all experiments except for the spike-triggered averaging paradigm (see below).

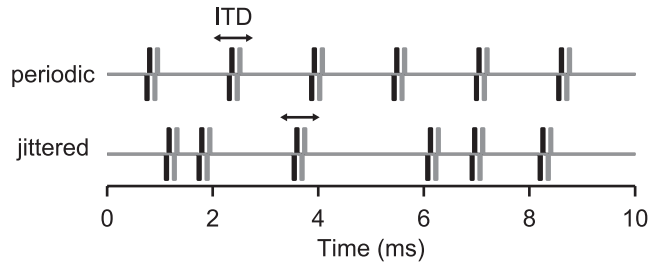

Fig. 1. Segments of periodic and jittered pulse trains with identical mean pulse rates. Black and gray traces distinguish stimuli to the two ears. Jittered pulse trains have irregular intervals but are binaurally coherent (same pattern presented to each ear). Jittered intervals are typically drawn from a uniform distribution spanning ±90% of the mean interpulse interval. ITD, interaural time difference.

Pulse trains were generated using 16-bit digital-to-analog converters (PXI-6221, National Instruments) and delivered to each CI through a pair of custom-built, isolated current sources. Stimulation was between the most apical and most basal intracochlear electrodes (separation: 5.25 mm). This wide bipolar electrode configuration allows stimulation of auditory nerve fibers innervating the entire length of the cochlea while minimizing stimulus artifacts relative to monopolar stimulation (Litvak et al. 2001).

Single-unit recording. Recordings were made from well-isolated single units using 16-site multichannel electrodes (Neuronexus). Signals were preamplified (TDT RA16) and then filtered (300–3,000 Hz) and amplified (×10,000) using a digital signal processor (TDT Medusa). The recording was typically performed differentially between adjacent electrodes in the array to minimize the amplitudes of stimulus artifacts and local field potentials. The conditioned signals were digitized at 100 kHz using a high-speed analog-to-digital converter (PXI-6123, National Instruments).

Artifact cancellation and spike detection were performed online using custom software. Artifact cancellation consisted of zeroing the electrode signal for a short interval (300–500 μs) after each stimulus pulse. Although a spike contained entirely within the cancellation window would be undetected by this method, the window is sufficiently short that, with good single-unit isolation, some portion of the spike waveform outside the cancellation window typically exceeds the discriminator threshold, allowing the spike to register with a small error in timing. Nevertheless, some spikes remained undetected with jittered stimuli at the higher pulse rates when the interpulse intervals could be shorter than the width of the cancellation window, resulting in an underestimation of firing rates in this condition.

Upon isolating a single unit, we first measured the threshold for single diotic pulses (ITD = 0). Subsequent measurements were made at 1–4 dB above the single-pulse threshold. Neural responses were measured as a function of pulse rate for both periodic and jittered pulse trains using diotic stimuli (ITD = 0). Pulse rate was varied in half-octave steps between 20 and 1,280 pps. A random pulse rate was selected on each stimulus presentation, and every pulse rate was presented 8–12 times. The maximum pulse rate was limited to 1,280 pps by the gating technique for stimulus artifact cancellation.

Neural ITD sensitivity was characterized by varying ITD from −2 to +2 ms in 200-μs steps, where contralateral-leading ITDs are positive. ITD was selected randomly on each stimulus presentation, and each was presented 8–12 times. This paradigm was repeated for

periodic and jittered conditions, using as many pulse rates as time permitted.

Data analysis. To compute average firing rate as a function of either pulse rate or ITD, the onset response was removed by excluding spikes occurring within the shortest time window lasting ≥15 ms and containing an integer number of interpulse intervals. Firing rates were computed by counting spikes over the remainder of the 300-ms pulse train duration. The rate window was chosen to ensure that the rate was computed over an integer number of pulse intervals in each case.

Clustering analysis. There was considerable variability among neurons with respect to how firing rate depends on stimulus pulse rate and the effectiveness of pulse train jitter. A *k*-means clustering analysis (kmeans, MATLAB) was used to analyze this variability and to objectively segregate neurons showing a pronounced sensitivity to jitter from those that do not. For each neuron, firing rate versus pulse rate curves in response to periodic and jittered stimuli were concatenated to form a single vector, which was then normalized by its maximum value. Response vectors are initially grouped at random into *k* clusters. The *k*-means procedure then iteratively reclusters the vectors to minimize the summed Euclidean distance between each vector and its cluster centroid. The entire clustering procedure was repeated 10 times with different random initial clusters to increase the likelihood of finding the global maximum. The number of clusters *k* is an independent variable that was systematically varied from 1 to 20.

ITD sensitivity metric. We used an ANOVA metric to characterize ITD sensitivity independently of the shapes of the ITD tuning curves (Hancock et al. 2010). This metric was derived from the raw spike counts (firing rates) for each ITD and each stimulus trial. Specifically, the "ITD signal-to-total variance ratio (STVR)" was defined as the ratio of the variance in firing rates attributable to changes in ITD to the total variance in firing rates. The latter can be expressed as the sum of the variance attributable to variations in ITD plus the variance across stimulus trials for each ITD (the "neural noise"). This metric captures the degree to which the variation in rate caused by changes in ITD dominates the variability in rate that occurs over multiple repetitions of a stimulus. It ranges between 0, indicating no ITD sensitivity, to 1, indicating perfectly reliable ITD coding across trials. Neural responses are said to be ITD sensitive when the ITD STVR is significantly greater than 0 ($P < 0.025$). This metric is the same as used in Hancock et al. (2010) except we have changed the name from "signal-to-noise ratio" to more accurately describe the computation. Like mutual information, the STVR characterizes ITD sensitivity without making any assumption about the nature of the neural code, but its accurate estimation requires fewer stimulus repetitions than mutual information because it depends only on variances of the spike counts rather than probability density functions.

Synchrony analysis. Synchrony between neural spikes and stimulus pulses was quantified using cross-correlation (e.g., Fig. 10). A cross-correlation histogram was constructed by binning the intervals between each stimulus pulse and every subsequent neural spike (bin width: 0.1 ms) up to a delay of 25 ms. Properly scaled, this cross-correlogram represents the average firing rate as a function of time, given that a stimulus pulse occurs at $time = 0$. Perfectly pulse-locked responses would yield a single nonzero bin at the spike latency, whereas completely unsynchronized responses would produce a flat cross-correlogram. Intermediate degrees of synchrony produce cross-correlogram peaks of variable height and width.

Confidence bounds were computed by Monte Carlo simulation for each cross-correlogram to assess whether its shape deviated significantly from that expected for a random spike train. The histogram computation was repeated 1,000 times using synthetic random spike trains, where the number of synthetic spikes was equal to the number of spikes in the actual neural response. Synthetic spike times were drawn randomly from a uniform distribution, excluding the 0.3- to 0.5-ms artifact gating window after each stimulus pulse during which spikes cannot be detected. The confidence bound on each bin was the 99th percentile of these synthetic cross-correlograms (see Fig. 10, gray shading). A cross-correlogram peak was regarded as significant when at least two consecutive bins exceeded the 99% confidence bounds.

Spike-triggered averaging of interpulse intervals. In some neurons, we used spike triggered averaging to shed light on which specific stimulus events trigger spike responses to high-rate jittered pulse trains. The basic strategy was to stimulate the neuron diotically with a long "training" pulse sequence comprising a nonrepeating, jittered pulse train. A continuous representation of the stimulus interpulse intervals was created, whose value at any point in time was the interval between the most recent pair of stimulus pulses. For example, if consecutive stimulus pulses occurred at times t_1, t_2, and t_3, the interpulse interval waveform equals $t_2 - t_1$ between times t_2 and t_3. The 20-ms segments of this waveform preceding each spike were averaged. As described fully in RESULTS, the spike-triggered average interpulse interval was used to predict the neural response to a "test" jittered pulse train token. The prediction was compared with the measured neural response to many repetitions of the test token.

In practice, test and training stimuli were interleaved to minimize the effect of rate trends on the analysis. The stimulus consisted of 61 independently generated jittered pulse train tokens, each 1 s in length. One token was selected as the test token, with the remaining 60 comprising the set of training tokens. Stimulation alternated between the test token and members of the training set. The combined set was presented twice, yielding 120 repetitions of the test stimulus and 120 s of training data. Stimulation was continuous (no off period between tokens) to eliminate onset effects from the response to each token.

RESULTS

Jitter can restore ongoing firing at high pulse rates. We measured responses as a function of pulse rate for both periodic and jittered pulse trains from 197 single units in the IC of acutely deafened (57 units), long-term adult-deafened (84 units), and congenitally deaf cats (62 units). The vast majority of neurons responded in an ongoing fashion to periodic pulse trains only for low pulse rates (less than ~100 pps) and gave an onset response at high pulse rates. For many neurons, however, pulse train jitter restored ongoing firing at high pulse rates.

Figure 2 shows the responses of two neurons, one sensitive to jitter (*top*) and one not (*bottom*). The jitter-sensitive neuron (Fig. 2, *A–C*) responded to low-rate periodic stimulation with pulse-locked firing (indicated by the regularly spaced dot patterns). Ongoing firing disappeared at higher pulse rates such that only onset spikes were observed >320 pps. This pattern of response to periodic electric pulse trains is typical of IC neurons in anesthetized preparations (Middlebrooks and Snyder 2010; Smith and Delgutte 2007a; Snyder et al. 1995). In response to jittered stimulation, spikes were precisely locked to each pulse at low pulse rates, as with periodic stimulation, but the firing rate declined less with increasing pulse rate, and the neuron fired robustly up to at least 1,280 pps, the highest pulse rate tested. Importantly, the temporal firing patterns evoked by high-rate jittered pulse trains were characterized by sparse preferred times of firing rather than randomly occurring spikes (Fig. 2*C*, *top*). Such preferred firing times are a general characteristic of responses to high-rate jittered pulse trains; the stimulus events giving rise to the preferred firing times are analyzed in detail in a later section.

In contrast, the neuron shown in Fig. 2, *D–F*, responded in an ongoing fashion only for very low pulse rates (≤40 pps). In this case, jittering the pulse train did not substantially change the rate response relative to periodic stimulation.

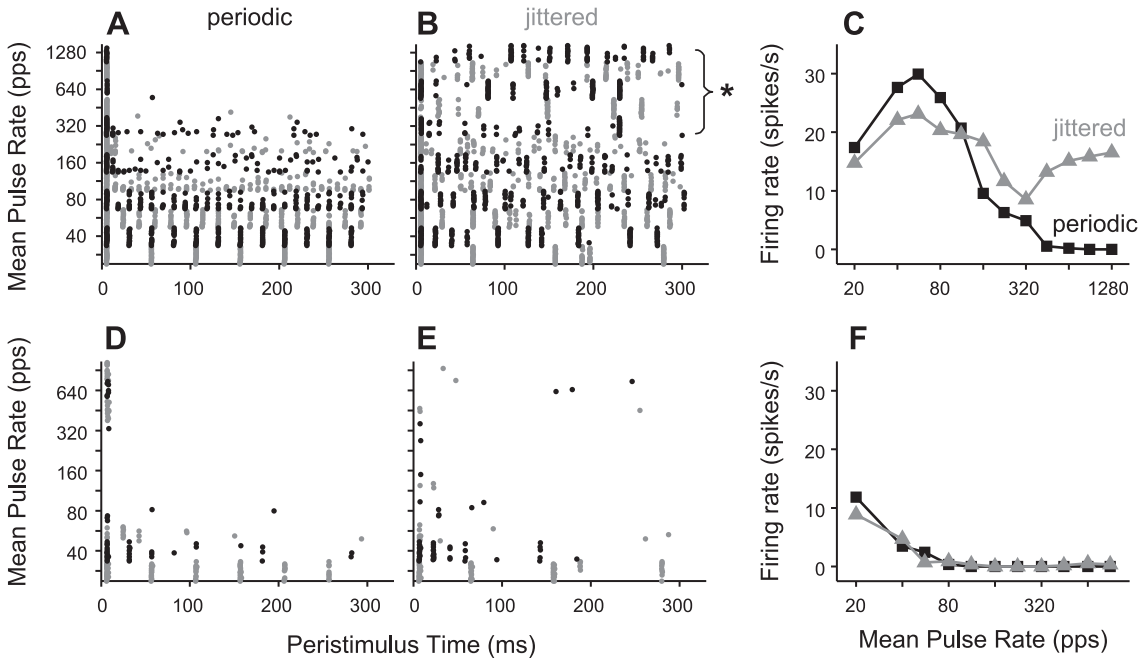

Fig. 2. Single-unit examples show variable sensitivity to pulse train jitter. *Top*: jitter-sensitive neuron. *Bottom*: jitter-insensitive neuron. Dot rasters show temporal firing patterns in response to periodic (*A* and *D*) and jittered (*B* and *E*) pulse trains. Alternating colors distinguish blocks of trials at different pulse rates. *C* and *F*: corresponding rate-vs.-pulse rate curves. Jitter restored ongoing firing to high pulse rates for the neuron at the *top* but not at the *bottom*. Responses to repeated presentations of high-rate jittered stimuli were characterized by sparse, preferred firing times (* in *B*). pps, pulses/s.

Clustering. The examples shown in Fig. 2 represent extremes in a continuum of relative sensitivity to pulse rate and jitter among our sample of IC units. We used *k*-means clustering to analyze the underlying variability (see METHODS). The percentage of the variance explained by the clustering increased smoothly with the number of clusters (Fig. 3*B*). Although the absence of a break point suggested that there was no "natural" number of clusters, $k = 5$ accounted for over half the variance, and we chose that number to illustrate the range of behavior. The cluster centroids (normalized rate-vs.-pulse rate functions averaged across cluster members) are shown in Fig. 3*A*. The numbers at the *top* of Fig. 3*A* indicate the percentage of neurons falling in each cluster.

The five clusters could be further grouped into two broad classes that differed in the pulse rate limit for sustained responses and sensitivity to jitter. "Sluggish" neurons (*clusters*

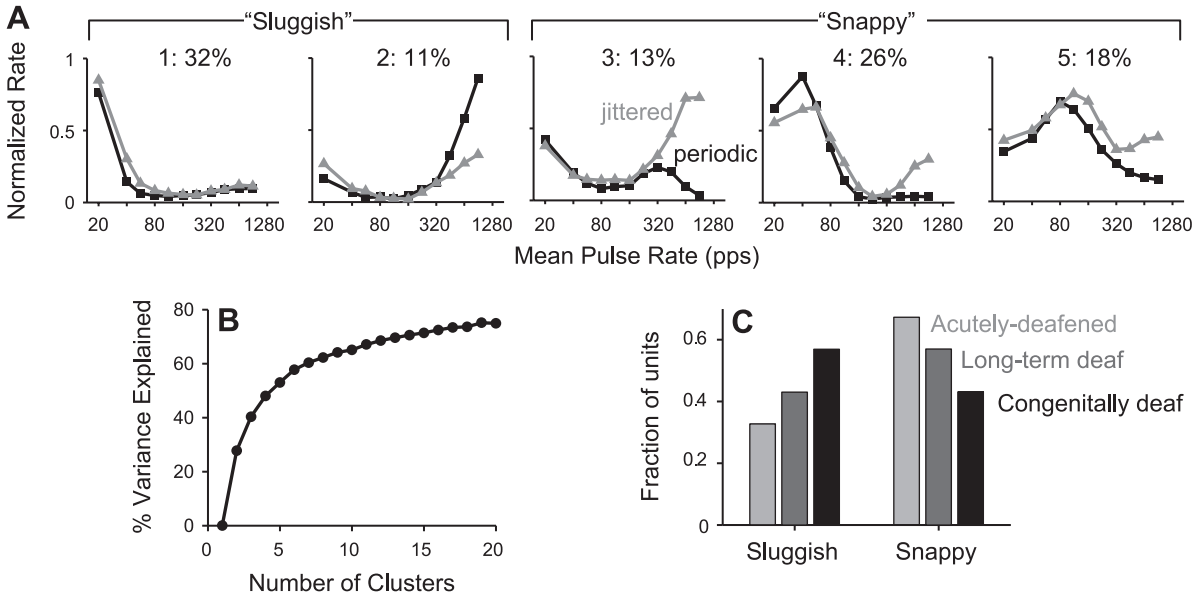

Fig. 3. Clustering analysis shows variable sensitivity to pulse train jitter across population. *A*: neurons were segregated into five clusters by applying a *k*-means procedure to normalized rate-vs.-pulse rates curves for periodic and jittered stimuli. For each neuron, rate was normalized by the maximum across all pulse rates and periodic/jittered conditions. Shown are the cluster centroids (average response of the neurons in each cluster). Percentages indicate the fraction of neurons assigned to each cluster. Further combination led to the "sluggish" and "snappy" categorizations, as shown. Snappy neurons showed a benefit of jitter at high-pulse rates and were sensitive over a larger range of low pulse rates. *B*: percent variance explained increases smoothly with the number of clusters, suggesting that responses vary across a continuum. *C*: the incidence of snappy responses depended on the onset age and duration of deafness.

1 and *2*) respond only at very low pulse rates (≤20 pps) and show similar or lower firing rates for jittered stimuli compared with periodic stimuli at high pulse rates. Most sluggish neurons (*cluster 1*) had responses similar to the example shown in Fig. 2*B*, showing no recovery of ongoing firing at high pulse rates for either periodic or jittered pulse trains. However, a quarter of the sluggish neurons (*cluster 2*) showed ongoing spike responses to high-rate jittered pulse trains but even greater responses to high-rate periodic pulse trains. The vast majority of *cluster 2* responses (~80%) occurred in congenitally deaf cats, where spontaneous activity and rebound responses are common (Hancock et al. 2010).

"Snappy" neurons (*clusters 3–5*) have sustained responses to periodic pulse trains over a larger range of low pulse rates and show a pronounced effect of jitter, especially at high pulse rates. The three snappy subclusters were qualitatively similar, only differing in the range of low pulse rates to which they were sensitive.

The relative incidence of sluggish and snappy responses varied systematically with the onset and duration of deafness (Fig. 3*C*). Snappy responses were most common in acutely deafened cats, less common in long-term adult-deafened cats, and least common in congenitally deaf cats. These trends were significant ($P < 0.01$ by χ^2-test).

Figure 4 shows the effects of pulse rate and jitter on the incidence of sustained firing among sluggish and snappy neurons. A neuron was classified as having a sustained response at a particular pulse rate if its steady state firing rate was >5 spikes/s. In general, the incidence of sustained firing had a bimodal distribution as a function of pulse rate, reflecting the tendency for IC neurons to have distinct low- and high-pulse rate regions of activity (e.g., Figs. 2*B* and 3*A*). For the sluggish group, the border between the two regions occurred at a relatively low pulse rate (~112 pps). Jitter increased the number of sluggish neurons with sustained responses in the low-pulse rate region, although the effect just missed significance ($P = 0.054$ by χ^2-test). At high pulse rates, jitter produced an insignificant reduction in the incidence of sustained responses ($P = 0.91$ by χ^2-test).

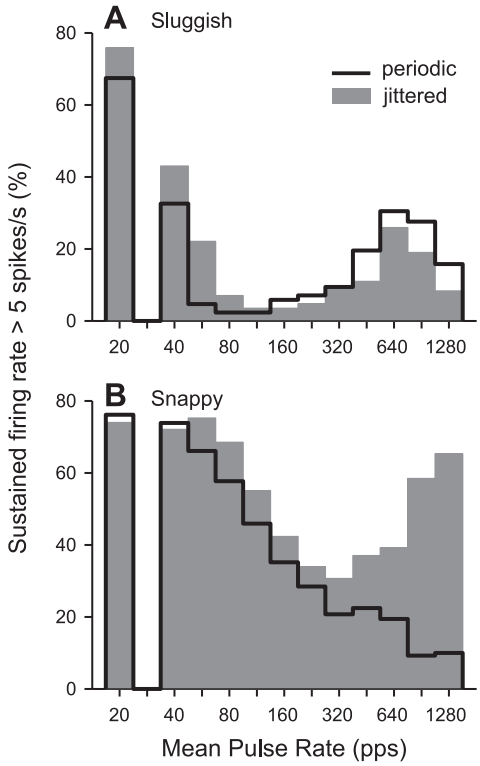

Fig. 4. Jitter increases the fraction of snappy neurons giving sustained responses to high pulse rates relative to periodic stimulation. Histograms show the incidence of sustained responses in sluggish (*A*) and snappy (*B*) neurons. The response was classified as sustained when the steady-state firing rate was >5 spikes/s.

Sustained firing was much more common at all pulse rates in the snappy group compared with the sluggish group. The transition between the two pulse rate regions was apparent only in the responses to jittered stimuli but clearly occurred at a much higher pulse rate (~320 pps) than in the sluggish group. In the low-pulse rate region, jitter produced a small increase in sustained activity among snappy neurons, but the effect was not significant ($P = 0.97$ by χ^2-test). Most importantly, for pulse rates >320 pps, jitter dramatically increased the number of snappy neurons giving sustained responses ($P < 0.001$ by χ^2-test).

Jitter restores ITD sensitivity in sustained-responding neurons. Ongoing responses evoked by high-rate jittered stimuli were ITD sensitive in a manner consistent with the responses to low-rate periodic stimuli. This is shown in Fig. 5*A* for the same neuron shown in Fig. 2, *A–C*. The rate-ITD curve for a 40-pps pulse train was peak shaped with a best ITD (the ITD giving rise to the maximum firing rate) near zero. The response was highly ITD sensitive, as indicated by the large ITD STVR (0.82; see METHODS). The rate-ITD curve for a 640-pps jittered pulse train also showed a peak near zero and was comparable in width but was more compressed, having both a smaller peak and elevated activity at unfavorable ITDs. Consequently, its ITD STVR was lower (0.60). The corresponding dot raster in Fig. 5*A* suggests that the reason for the compressed shape is that ITD modulates spiking for only a subset of the sparse, preferred firing times. Specifically, the spikes occurring at ~80 and ~200 ms occurred for all ITDs, whereas the spikes at ~110 and ~150 ms were more strongly modulated by ITD. In contrast, ITD tuning evoked by periodic stimulation tended to be less variable over the duration of the sustained response, when present (Hancock et al. 2010; Smith and Delgutte 2007a).

Figure 5, *B* and *C*, shows example responses from two other snappy neurons. As shown in Fig. 5*A*, there were no sustained responses to the high-rate periodic pulse train in these neurons, and jitter restored ongoing firing at the higher pulse rate, revealing ITD tuning qualitatively similar in shape and best ITD to that produced by low-rate stimuli. Also as shown in Fig. 5*A*, the dot rasters showed that ITD tuning differed across the different sparse firing times. The three representative examples shown in Fig. 5, *A–C*, differ primarily in their maximum firing rates and the relative ITD STVRs for jittered compared with low-rate periodic stimuli. In contrast, Fig. 5*D* shows the response of an unusual snappy neuron that responded robustly to both periodic and jittered high-rate pulse trains. ITD tuning was similar for both stimuli, consistent with the idea that the primary effect of jitter is to restore ongoing firing, but jitter had little influence on ITD coding per se.

Figure 6 shows a comparison of ITD STVR for high-rate jittered pulse trains and low-rate periodic pulse trains across our sample of IC units. The ordinate is the maximum STVR for any jittered pulse train with mean pulse rate ≥320 pps,

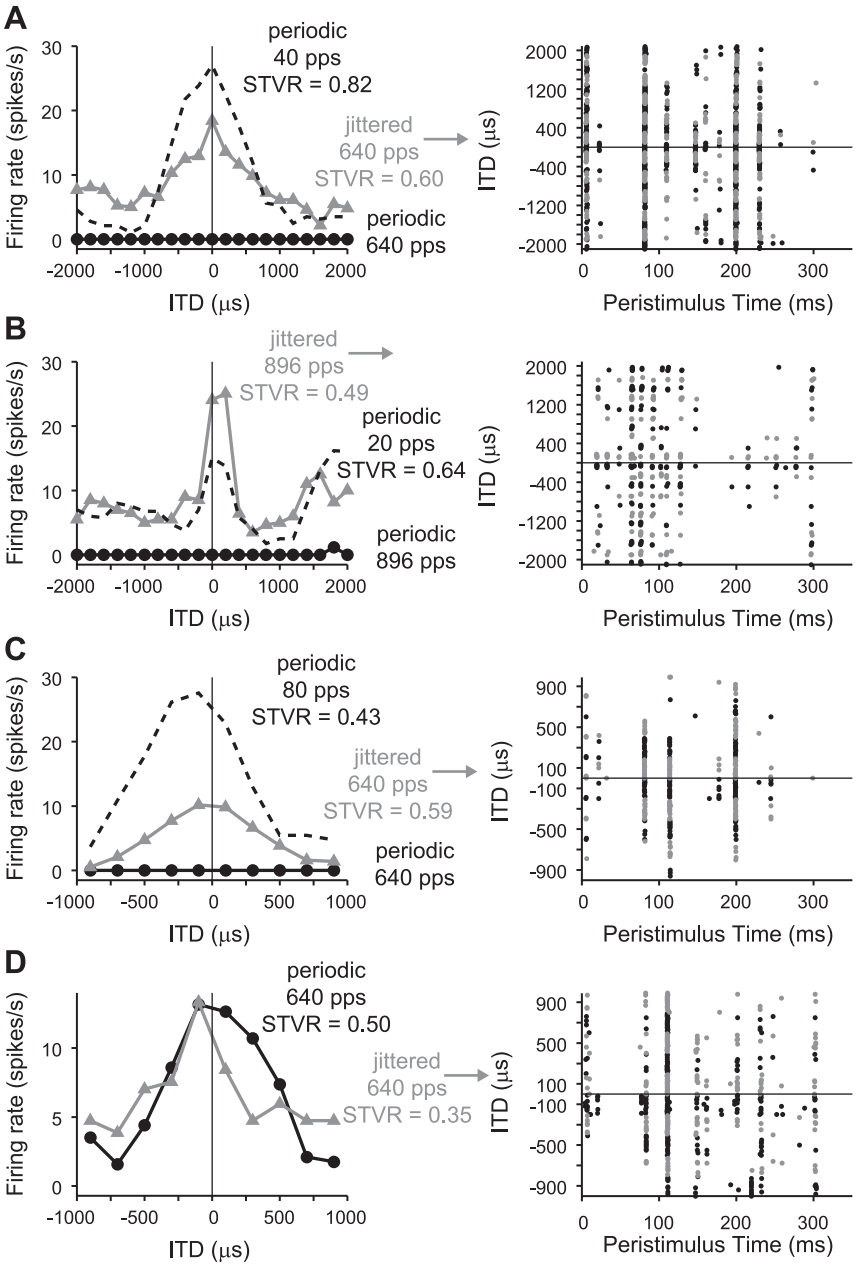

Fig. 5. Responses evoked by jittered high-rate pulse trains show ITD tuning comparable with that produced by low-rate periodic pulse trains. *Left*: rate-vs.-ITD curves. *Right*: dot rasters for the jittered, high-pulse rate condition exhibited sparse, preferred firing times. Alternating colors distinguish blocks of trials at different ITDs. All examples shown are from the snappy group. *A*-*C*: most neurons did not respond to high-rate periodic stimuli (black circles). Jitter restored ongoing firing at these rates (gray triangles), revealing rate-ITD curves similar in shape to those produced by low-rate periodic stimuli (black dashed lines). *D*: uncommon neuron that responded well to high-rate periodic stimuli. ITD tuning was similar for high-rate jittered and periodic pulse trains. *A*: long-term deafened cat. *B*: acutely deafened cat. *C* and *D*: congenitally deaf cats. STVR, signal-to-total variance ratio.

whereas the abscissa is the maximum STVR measured for any periodic pulse train ≤112 pps. A data point was included only if the ITD STVR was significantly greater than zero ($P < 0.025$) for either the jittered or periodic case. Most of the data points were below the equality line, meaning that ITD sensitivity was poorer for high-rate jittered pulse trains than for low-rate periodic pulse trains in the same neurons ($P < 0.001$ by paired *t*-test). Most of the sluggish neurons included in Fig. 6 belonged to *cluster 2*, which exhibits ongoing firing in response to both periodic and jittered high-rate stimuli.

Figure 7, *A* and *B*, shows the percentage of neurons showing significant ITD sensitivity for periodic and jittered stimuli as a function of pulse rate. The data were relatively sparsely sampled with respect to pulse rate because time allowed measurement of ITD sensitivity at only a few pulse rates for most neurons. There is an inherent bias in selecting these data in that neurons were tested for ITD sensitivity at a particular pulse rate only when ongoing firing could be evoked under at least one condition (periodic or jittered stimuli). The data thus do not reflect the prevalence of ITD sensitivity across the entire population at each pulse rate. Nevertheless, they indicate that, among the snappy neurons, for which jitter typically evokes ongoing firing at high pulse rates, most of the neurons thus activated were ITD sensitive, and this represents a substantial improvement over the periodic case. Sluggish neurons, in contrast, showed minimal effect of jitter on the prevalence of ITD coding at high pulse rates, consistent with the limited ability of jitter to enhance ongoing firing in these neurons. The increase in the fraction of ITD-sensitive sluggish neurons at 40 and 80 pps, although not significant ($P = 0.11$ by Fisher's exact test), was consistent with the jitter-related enhancement of sustained responses at those pulse rates (Fig. 4*A*).

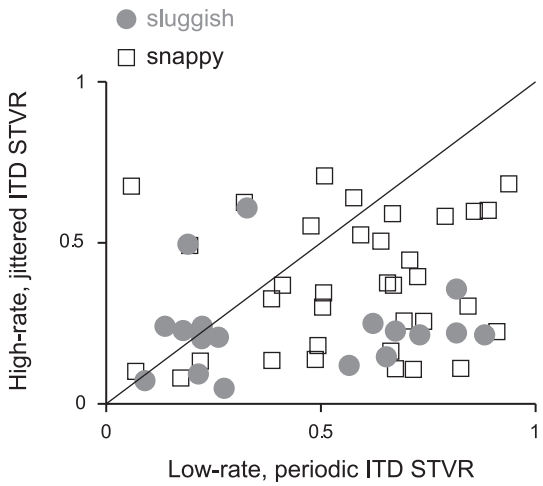

Fig. 6. ITD sensitivity is greater for low-rate, periodic pulse trains than high-rate, jittered pulse trains. Each point represents a single neuron. Sluggish and snappy classes are indicated separately.

Figure 7, *C* and *D*, shows mean ITD STVR (±SE) as a function of pulse rate for the same selection of data as shown in Fig. 7, *A* and *B*. In sluggish neurons, ITD STVR degraded with increasing pulse rate, and there was no difference between periodic and jittered pulse trains, for either low pulse rates (<320 pps, $P = 0.56$ by paired *t*-test) or high pulse rates (≥320 pps, $P = 0.55$ by paired *t*-test). ITD STVR in snappy neurons tended to be larger than in sluggish neurons and degraded with pulse rates only above 80 pps. For pulse rates ≥320 pps, where jitter has the largest effect on firing rate, the ITD STVR was significantly larger for jittered pulse trains than for periodic pulse trains ($P < 0.01$ by paired *t*-test).

We have suggested that jitter reveals the latent ITD sensitivity by restoring ongoing firing. If so, we expect that, in the few cases when high-rate periodic stimuli evoke ongoing firing (e.g., Fig. 5*D*), such responses would be as sensitive to ITD as responses evoked by high-rate jittered stimuli. Figure 7, *E* and *F*, confirms this prediction by showing the mean ITD STVR as a function of pulse rate only for responses with maximum ongoing firing rates >5 spikes/s. Although the majority (~70%) of responses to high-rate periodic stimuli were excluded by this criterion, the mean ITD STVR for the remaining few was comparable with that obtained with jittered stimuli (Fig. 7*F*). Interestingly, the mean ITD STVR for snappy neurons still showed two maxima separated by a minimum at 320 pps for both periodic and jittered stimuli when the influence of overall firing rate was eliminated by this thresholding.

We have demonstrated that the principal effect of pulse train jitter is to restore ongoing firing at high pulse rates. These ongoing responses showed similar ITD tuning as responses produced by low-rate periodic pulse trains, although generally with smaller ITD STVR. Next, we describe in more detail the effect of pulse train jitter on neural responses and explore the mechanisms by which jitter produces an effect by analyzing the temporal discharge patterns.

Substantial pulse train jitter is required to evoke a sustained response. In some neurons, the amount of jitter required to evoke a sustained response to a high-rate pulse train was measured by systematically varying the percent jitter. Figure 8 shows the response of the neuron shown in Fig. 2*A* to a 640-pps jittered pulse train as a function of percent jitter. Jitter <70% yielded only onset spikes (Fig. 8*A*). A weak ongoing response was produced starting at 70% jitter. Beyond that, the steady-state firing rate increased monotonically with increasing jitter (Fig. 8*B*). As in the other examples shown, reproducible spike patterns were observed with repeated presentation of jittered pulse trains that evoke ongoing firing (Fig. 8*A*).

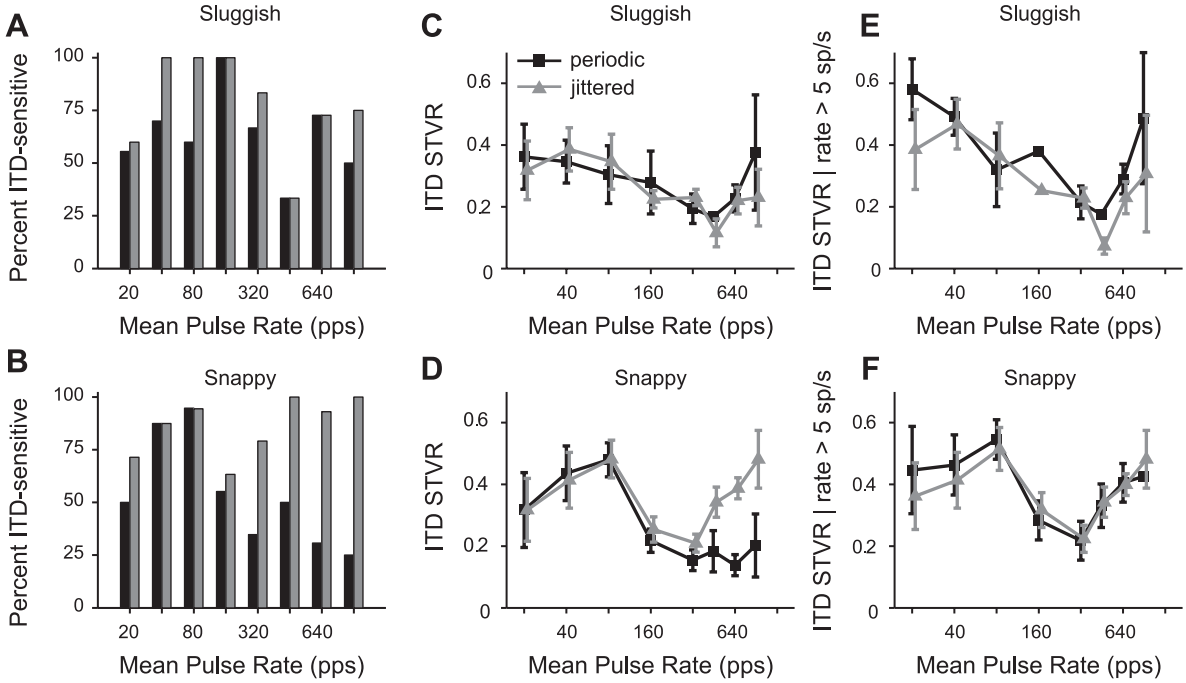

Fig. 7. Jitter improves ITD sensitivity at high pulse rates for snappy neurons. *A* and *B*: percentage of neurons sensitive to ITD as a function of mean pulse rate for periodic (black) and jittered (gray) stimuli. *C* and *D*: ITD STVR (mean ± SE) as a function of mean pulse rate. Jitter significantly improved the ITD sensitivity of snappy neurons to pulse rates ≥320 pps. *E* and *F*: ITD STVR (mean ± SE) limited to responses for which the maximum firing rate was >5 spikes/s. For the handful of snappy neurons responsive to high-rate periodic pulse trains, ITD sensitivity was equal to that produced by high-rate jittered stimuli.

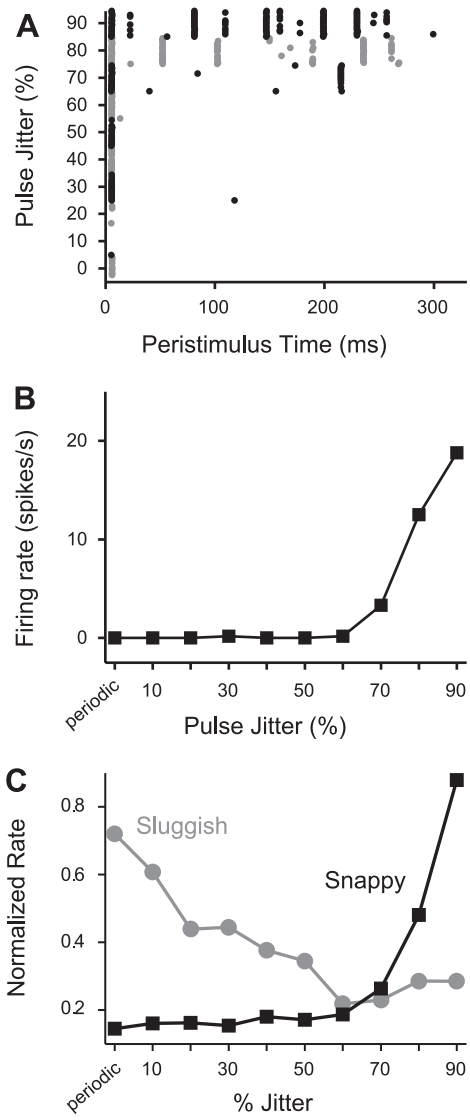

Fig. 8. Substantial pulse train jitter is required to elicit an effect. *A* and *B*: response of one neuron to a 640-pps pulse train as a function of percent jitter. *A*: dot raster. Alternating colors mark blocks of trials for different amounts of jitter. *B*: corresponding rate-vs.-percent jitter curve. At least 70% jitter was required to evoke ongoing firing in this neuron. *C*: normalized firing rate as a function of percent jitter, averaged across neurons within the sluggish (gray, $n = 12$) and snappy (black, $n = 20$) groups. On average, snappy neurons did not respond unless the pulse train was jittered by at least 70%.

The dependence on the amount of jitter illustrated by this example was typical of the snappy neuron group as a whole. Figure 8*C* shows the average normalized firing rate for sluggish and snappy neurons as a function of the amount of jitter. Firing rates were normalized by the maximum across all jitter amounts before being averaged. Data were pooled across pulse rates of 448, 640, and 896 pps. For snappy neurons, firing rate was not graded over the whole range; rather, there was a threshold at ~70% beyond which jitter became effective. In contrast, increasing jitter tended to decrease firing rates for sluggish neurons.

Sparse, preferred firing times reproduce across neurons. The dot raster patterns shown in Figs. 2, 5, and 8 show stereotyped responses in which repeated presentation of the same sequence of jittered pulses evokes spiking at highly reproducible times. Figure 9 demonstrates the generality of this behavior across the neural population. Peristimulus time histograms (PSTHs) were summed across all neurons within the sluggish and snappy groups. Pooled PSTHs for each group are shown as a function of mean pulse rate for both periodic and jittered stimuli. Sluggish neurons tended to have spontaneous activity and exhibited rebound responses, both after individual pulses at low rates and after the end of the pulse train at higher rates. Snappy neurons responded in a more precisely pulse-locked manner. The snappy neuron PSTHs for high-rate jittered stimuli were highly structured, consisting of several narrow, discrete peaks, indicating that responses to jittered pulse trains were reproducible across neurons as well as across trials.

Jitter-evoked responses are pulse locked. The reproducible preferred firing times evident in the single-unit dot rasters and pooled PSTHs suggest that there is some specific feature of the jittered pulse train that causes neurons to fire. We quantified the degree to which responses were locked to stimulus pulses by cross-correlating the neural spike trains with the stimulus pulse trains for both periodic and jittered stimuli. This analysis is more appropriate here than a conventional period histogram because jittered stimuli have no fixed period.

Figure 10 shows spike train/pulse train cross-correlograms for one snappy neuron, arranged by mean pulse rate. The cross-correlograms represent the mean instantaneous firing rate given the occurrence of a stimulus pulse at the time origin. The main features of the cross-correlograms are consistent with the data for mean firing rates presented above. Robust pulse-locked responses were evoked by low-rate stimuli, whether periodic or jittered. As pulse rate increased, neural spiking to periodic stimuli rapidly disappeared but was restored by jitter for pulse rates ≥448 pps. For low-rate stimuli, there was tight coupling between stimulus pulses and neural spikes, indicated by the prominent peaks in the cross-correlograms. Most stimulus pulses yielded a spike after a latency of ~5 ms. Responses evoked by high-rate jittered pulse trains were also stimulus locked, as shown by the significant cross-correlogram peaks, with similar latencies as for low-rate pulse trains. The presence of these cross-correlogram peaks shows that the ongoing responses produced by jitter do not just reflect a general increase in excitability but rather that spikes tend to be preceded by specific stimulus pulses. The converse is not true: not every stimulus pulse evoked a spike, and hence the cross-correlogram showed a nonzero baseline, reflecting either nonpulse-locked spikes or spikes evoked by intervening stimulus pulses occurring at times other than the origin of the correlogram.

Pulse-locked responses were common when jitter evoked ongoing firing at high pulse rates. The histograms shown in Fig. 11 plot the fraction of neurons for which the response was pulse locked, where a response was classified as pulse locked if the cross-correlogram contained a peak significantly above the noise floor (see METHODS). To quantify the effect of jitter on pulse locking per se, separate from its effect on ongoing firing, the analysis shown in Fig. 11 was limited to responses for which the ongoing firing rate was >5 spikes/s. As expected, pulse-locked responses were much more common among snappy neurons than among sluggish neurons. For snappy neurons, the fraction of pulse-locked responses to periodic stimuli decreased rapidly with increasing pulse rate between 80 and 640 pps. In contrast, the fraction of pulse-locked responses

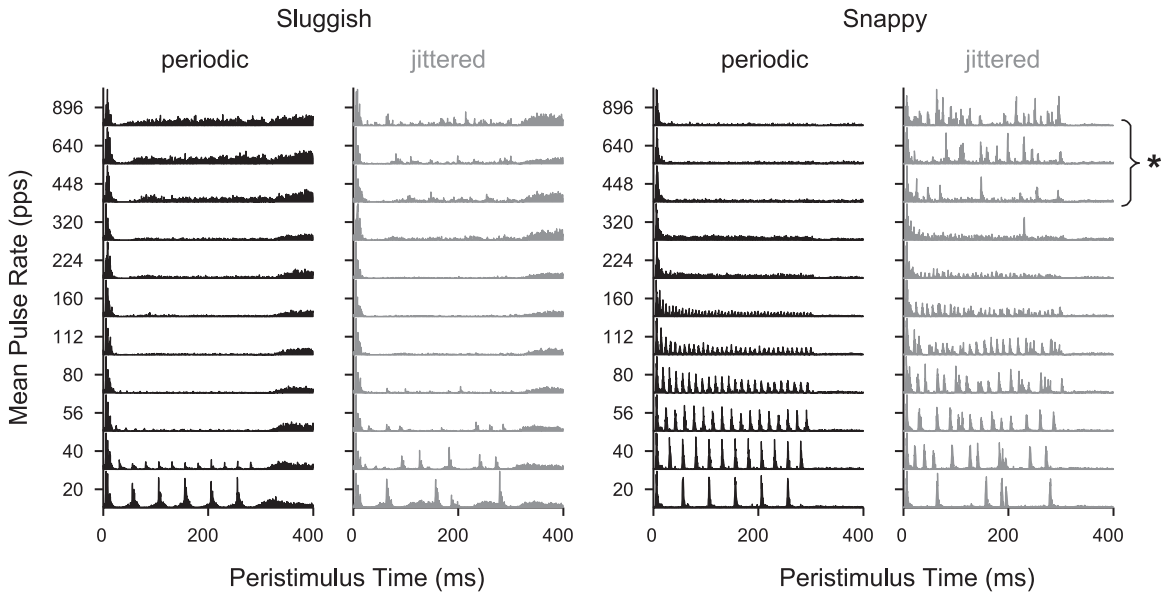

Fig. 9. Peristimulus time histograms (PSTHs) pooled across neurons within the sluggish (*left*) and snappy (*right*) groups. Sluggish neurons responded only to the lowest pulse rates tested (in the low-pulse rate region) and were minimally affected by jitter. Snappy neurons responded over a larger range of low pulse rates and exhibited a pronounced effect of jitter at high pulse rates. The sparse, preferred firing times were reproducible across neurons (*).

to jittered stimuli among snappy neurons did not drop as sharply, and over half of the these neurons retained pulse-locked responses to 1,280 pps jittered stimuli if they had an ongoing response. Jitter significantly increased the fraction of pulse-locked responses among snappy neurons ($P < 0.001$ by χ^2-test) but not sluggish neurons ($P = 0.5$ by χ^2-test).

As expected, ongoing responses to high-rate, periodic pulse trains did not need to be pulse locked to be ITD sensitive (compare Figs. 11*B* and 7*F*). This is consistent with responses to pure tones in normal hearing animals, where only a fraction of IC neurons that are ITD-sensitive phase lock to monaural pure tones at their best frequency (Kuwada et al. 1984).

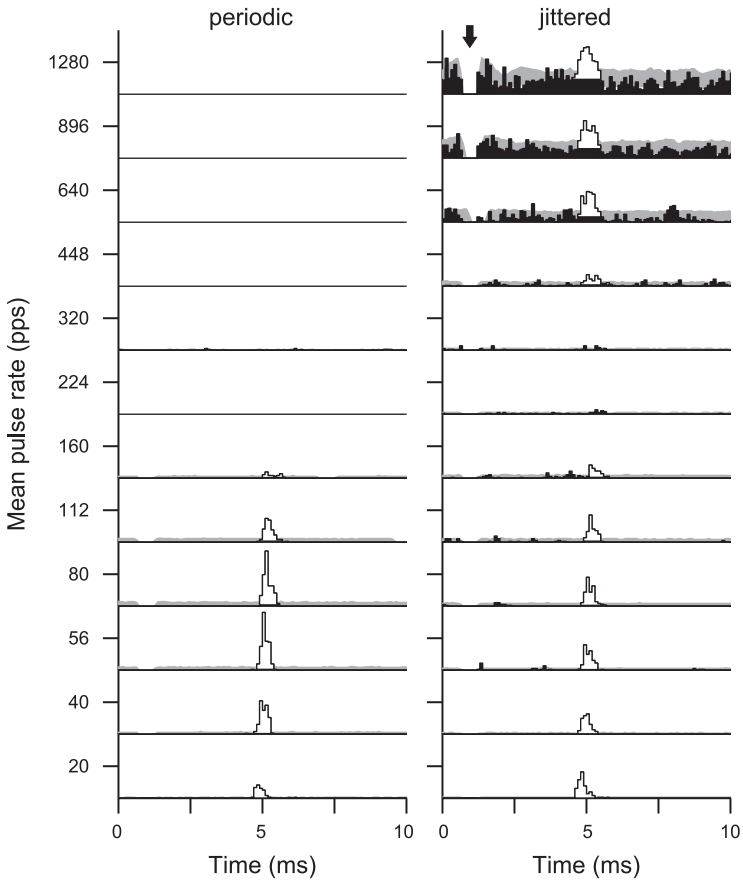

Fig. 10. Pulse locking quantified by cross-correlating neural spike trains with stimulus pulse trains. Data shown are from example snappy neuron. Cross-correlograms (black bars) plot probability of neural firing as a function of time given a stimulus pulse at time = 0. Gray shading indicates 99% confidence bounds estimated from a Monte Carlo simulation. Peaks exceeding the confidence bounds indicate significant pulse locking and are open. This method is advantageous because it applies to both periodic and jittered stimuli and is insensitive to gaps introduced by stimulus artifact gating (arrow).

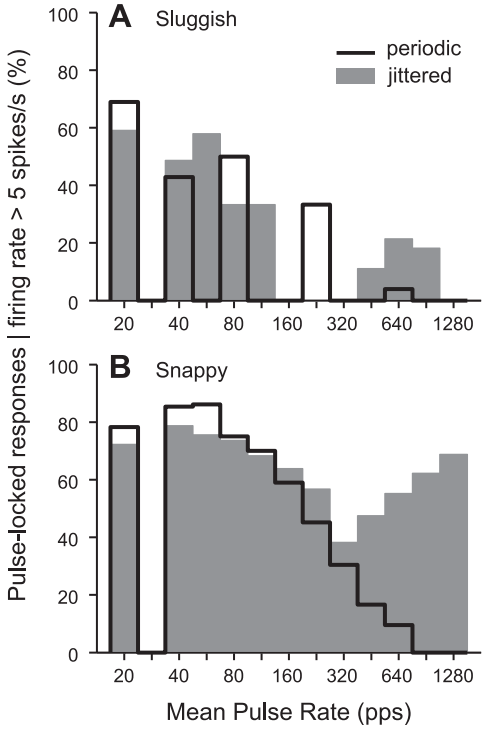

Fig. 11. Percentage of neurons that showed significant pulse locking at each pulse rate. Responses were included only if the ongoing firing rate was >5 spikes/s to isolate the effect of jitter on pulse locking. Pulse locking was much more common among snappy neurons. *A*: jitter had a minimal effect on pulse locking by sluggish neurons. *B*: jittered, high-rate pulse trains evoked pulse-locked ongoing firing by snappy neurons.

Jitter-evoked responses are triggered by short interpulse intervals. High-rate jittered pulse trains evoke ongoing responses characterized by sparse, preferred firing times, as demonstrated by the dot raster patterns shown in Figs. 2, 5, and 8 and the pooled PSTHs shown in Fig. 9. Moreover, the cross-correlation analysis shown in Figs. 10 and 11 shows that these sparse responses were tightly coupled in time to specific stimulus pulses. These observations together suggest that neurons respond to specific features of jittered pulse trains.

Two such specific features have been hypothesized, based on the fact that jittered pulse trains comprise sequences of relatively long and short interpulse intervals. One possibility is that firing to a stimulus pulse tends to occur after a long interpulse interval that allows recovery from adaptation or refractoriness (van Hoesel 2008a). Alternatively, temporal summation of postsynaptic potentials after short intervals may produce membrane depolarizations that transiently exceed a neuron's adapted threshold (Goupell et al. 2010).

We used spike triggered averaging to test which, if either, of these hypotheses best accounted for the neural data. For nine neurons, we computed a spike-triggered average of the instantaneous interval between the two most recent stimulus pulses in response to 120 s of continuous jittered stimulation. One such spike-triggered average is shown in Fig. 12*A*, where the abscissa represents time preceding a spike and the ordinate represents the instantaneous pulse rate (i.e., the reciprocal of the instantaneous interpulse interval). On average, each spike was preceded by a large, transient increase in the instantaneous pulse rate above the mean pulse rate (640 pps, solid horizontal line). The latency of the transient increase was ~5 ms, consistent with the latency estimated from the cross-correlogram for this neuron (not shown).

All nine neurons tested yielded similar spike-triggered averages, suggesting that spike responses to high-rate jittered pulse trains are evoked specifically by short interpulse intervals. The spike-triggered averages typically peaked at approximately four times the mean pulse rate, meaning that neurons responded preferentially to pairs of stimulus pulses for which the interpulse interval was less than a quarter of the mean. Interestingly, at least 75% jitter was required to produce intervals this short, consistent with the dependence of firing rate on percent jitter measured directly in Fig. 8.

As a further test of the short-interval hypothesis, we attempted to predict the response of the neuron shown in Fig. 12 to a 1-s jittered pulse train token not included among those used to generate the spike-triggered average. Figure 12*B* shows a segment of this "test" pulse train, where vertical lines represent individual stimulus pulses and the line heights indicate the instantaneous pulse rate (the reciprocal of the preceding interpulse interval). This representation of the pulse train was thresholded at the peak amplitude of the spike-triggered average shown in Fig. 12*A* (2,500 pps). The difference between instantaneous pulse rate and threshold was half-wave rectified and convolved with a Gaussian function (latency: 5 ms, SD: 0.5 ms) introduced to simulate neural spike latency and variability in spike timing (Hancock et al. 2010). Figure 12*C* shows a comparison of the resulting predicted PSTH with the PSTH measured from 120 repetitions of the test token. The short-interval hypothesis accurately predicted the preferred firing times and, to a lesser extent, the relative amplitudes of the individual PSTH peaks. The correlation coefficient between the measured and predicted PSTHs was 0.65.

The short-interval hypothesis also predicted the pooled responses of snappy neurons to high-rate jittered pulse trains, as shown in Fig. 13. Predictions were generated by thresholding the stimulus pulse trains and convolving with a Gaussian function, as described above, for mean pulse rates of 448, 640, and 896 pps. In each case, the threshold was set to four times the mean pulse rate. For the most part, the timing of the main peaks in the predicted PSTH was in good agreement with that in the measured pooled PSTH. The success of these predictions demonstrates that peaks in the pooled PSTHs tended to occur at times corresponding to the very shortest interpulse intervals in the stimulus.

DISCUSSION

In anesthetized cats, IC neurons encode the ITD of intracochlear electrical pulse trains only for pulse rates up to ~100 pps (Smith and Delgutte 2007a). This limitation is likely a consequence of the fact that IC neurons respond in an ongoing fashion only over a similar range of pulse rates (Middlebrooks and Snyder 2010; Snyder et al. 1995). Here, we show that imposing binaurally coherent jitter on the interpulse intervals restores ongoing firing at high pulse rates (≥320 pps) in about half of IC neurons, thereby revealing latent ITD sensitivity.

We used a clustering analysis to characterize the variability across the IC neuron population with respect to dependence on pulse rate and sensitivity to jitter. The clustering was used to segregate responses into two broad classes. Sluggish neurons show sustained responses only at very low pulse rates and have

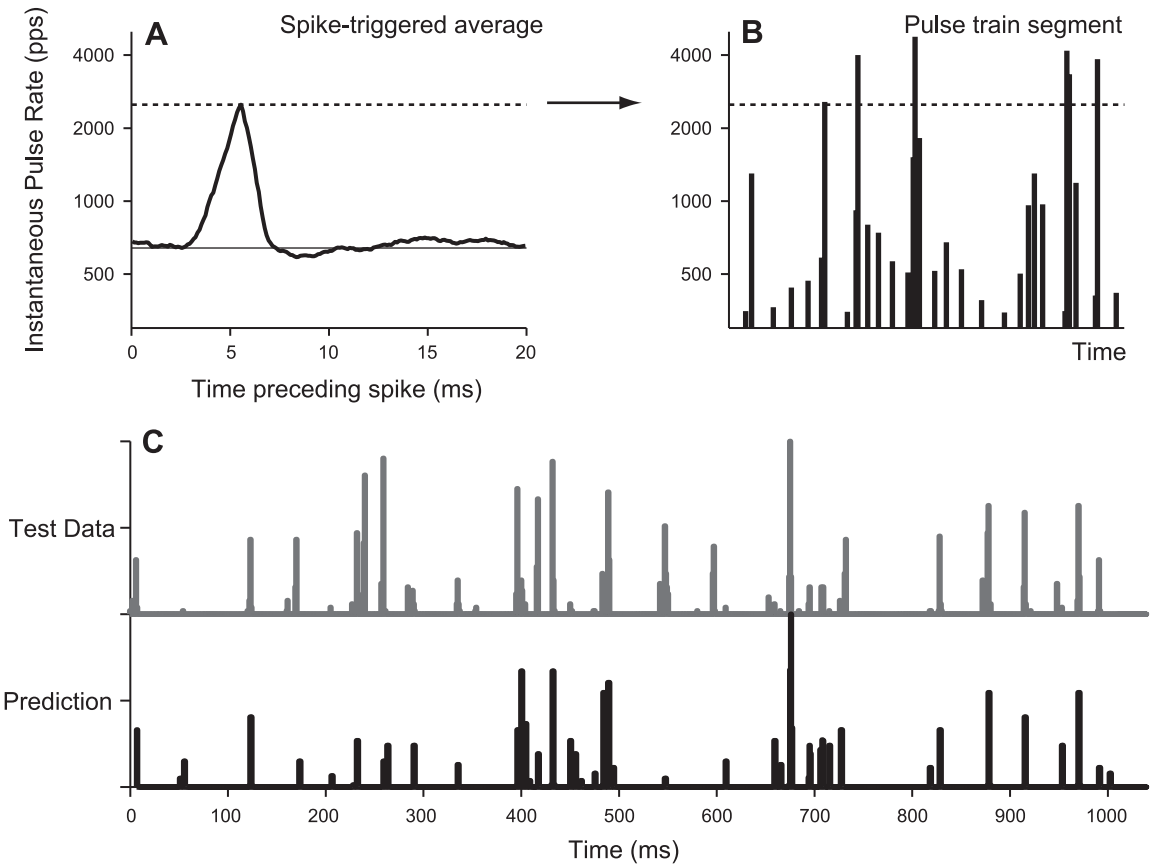

Fig. 12. Short interpulse intervals mediated the effect of jitter on the response of this neuron. *A*: spike-triggered average of the instantaneous stimulus pulse rate in response to 120 s of continuous (nonrepeating) jitter. The average neural spike was preceded by a rapid increase in pulse rate (i.e., short interpulse intervals). The horizontal line shows the mean stimulus pulse rate (640 pps). *B*: generation of a predicted response to an independent 1-s jittered pulse train token. Vertical lines represent individual stimulus pulses. Line heights indicate the instantaneous pulse rate (the reciprocal of the preceding interpulse interval). Pulse train thresholded at the peak amplitude of the spike-triggered average (dashed line) and then rectified and smoothed. *C*: comparison of predicted and actual PSTHs in response to independent jitter token. The short interpulse intervals accurately predicted the sparse, preferred firing times.

minimal sensitivity to jitter, whereas snappy neurons respond at higher pulse rates and show pronounced jitter effects at high rates. Although the data shown in Fig. 3 suggest that responses actually form a continuum rather than discrete classes, it was nevertheless useful to distinguish jitter-sensitive neurons from insensitive ones to make parametric analyses and characterize the effect of jitter on ITD coding.

The relative proportion of snappy neurons depended on the duration and onset age of deafness (Fig. 3*C*), consistent with earlier data on the effect of neonatal deafening on the range of pulse rates over which IC neurons respond to periodic pulse trains (Snyder et al. 1995; Vollmer et al. 2005). The three deafness groups differed mainly in the prevalence of neurons belonging to each response cluster. There did not appear to be any dependence on duration or onset of deafness within clusters. Thus, subsequent analyses were segregated based on the two broad clusters rather than deafness group.

Some of the wide variability in our data might be caused by differences in the location of neurons along the tonotopic axis of the IC and, therefore, in the brain stem nuclei that neurons receive inputs from (Loftus et al. 2010). We sampled neurons across a wide range of the dorsal-ventral axis of the IC. Based on tonotopic maps of the IC in normal-hearing cats (Smith and Delgutte 2007b), we estimate that the sampled neurons would span an approximate characteristic frequency (CF) range of 200–35,000 Hz. Consistent with previous reports with electric stimulation (Smith and Delgutte 2007a; Hancock et al. 2010), the incidence of ITD sensitivity at low pulse rates did not obviously depend on location on the tonotopic axis. The upper rate limit for responses to periodic pulse trains and the effects of jitter showed no dependence on the depth of the recording site either.

Comparison with psychophysics. The effect of binaurally coherent jitter on neural ITD coding was broadly consistent with psychophysical data from human subjects with bilateral CIs (Laback and Majdak 2008). That study used percent correct left/right discrimination to quantify ITD discrimination as a function of mean pulse rate and amount of jitter. Performance was good with 400-pps periodic and jittered pulse trains and degraded with increasing pulse rate for periodic stimuli but remained good for jittered stimuli up to 1,515 pps. ITD discrimination improved systematically with increasing amount of jitter; as little as 25% jitter produced measurable improvement in performance.

Neural ITD sensitivity behaved in a qualitatively similar manner, with some quantitative differences in the pulse rates and percent jitter over which an effect of jitter was observed. Periodic and jittered stimuli both showed good ITD sensitivity for pulse rates less than ~100 pps, but ITD sensitivity in snappy neurons was improved by jitter for pulse rates >320

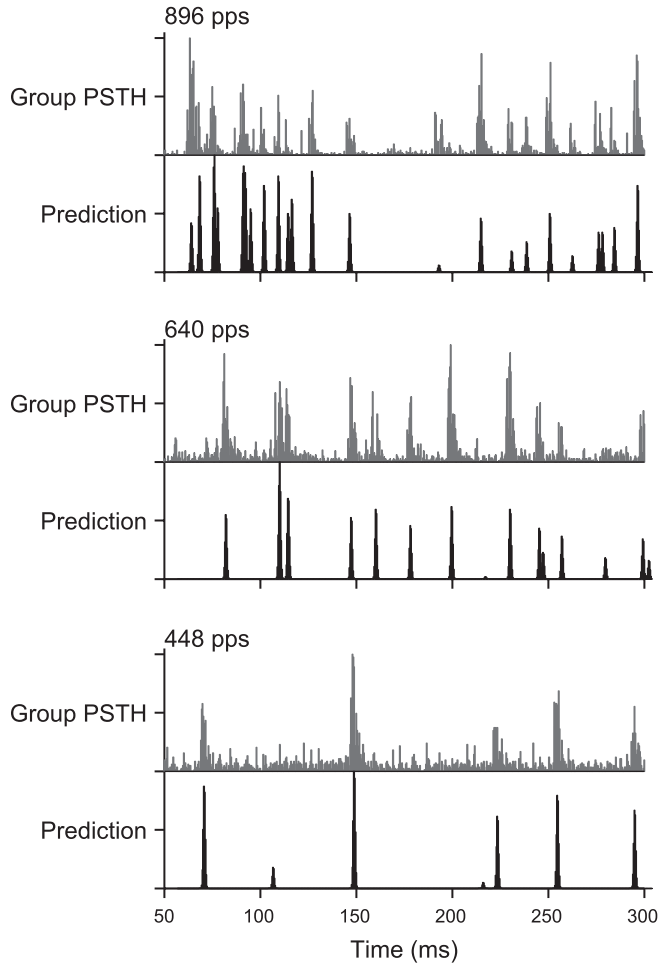

Fig. 13. Short interpulse intervals predicted the pooled responses to high-rate jittered pulse trains. Gray, subset of pooled PSTHs from Fig. 9; black, predicted PSTHs generated as in Fig. 12, *B* and *C*, using a threshold of four times the mean pulse rate. Peaks in the measured PSTHs occurred at times well predicted by the shortest interpulse intervals.

pps (Fig. 7*D*). Although ITD sensitivity was not directly characterized as a function of percent jitter, the ongoing firing that seems to be necessary for expressing ITD sensitivity systematically increased in rate with percent jitter. On average, at least 70% jitter was required to produce an ongoing response.

In deaf animals, jitter restores ongoing firing in ~40% of the IC neurons that do not respond to high-rate periodic stimulation. Our previous modeling analysis suggests that increasing the number of ITD-sensitive neurons by a similar fraction can improve perceptual ITD discrimination thresholds by an order of magnitude in response to low-rate periodic pulse trains (Hancock et al. 2010). On that basis, it appears that jitter affects a sufficient number of neurons to account for the magnitude of the jitter effect observed by Laback and Majdak (2008) in CI users.

The beneficial effects of jitter on ITD discrimination is observed not only in bilateral CI users but also in normal-hearing listeners when stimulated by high-rate click trains band-pass filtered around 4.6 kHz (Goupell et al. 2009). An effect of jitter on both ongoing responses and ITD sensitivity of IC neurons at high pulse rates was also observed in one normal-hearing cat (Goupell et al. 2010). The jitter effect was observed for neurons with CFs above 3 kHz, which are not sensitive to ITD in the temporal fine structure of noise stimuli (Devore and Delgutte 2010; Joris 2003). Thus, both neural and perceptual jitter effects are observed in normal hearing as well as with CIs.

Despite many similarities, the neural and behavioral data do differ with respect to the range of pulse rates over which the effects occur and the amount of jitter required to produce an effect. Differences in anesthetic state likely contribute to such differences. Specifically, upper pulse rate limits for ongoing firing in IC neurons have been shown to be substantially higher for awake compared with anesthetized animals with electric stimulation (Chung et al. 2012), and effects of anesthesia have also been demonstrated on ITD tuning of IC neurons in normal-hearing animals (Kuwada et al. 1989). Differences in stimuli may also contribute. Specifically, the psychophysical data were obtained using pulse trains amplitude modulated at 12.5 Hz by trapezoidal waveforms with slow (20-ms) ramps to minimize onset ITD cues. In contrast, we used unmodulated pulse trains and discarded the onset portion of the response to eliminate the contribution of onset ITD cues. Low-frequency amplitude modulation can restore ongoing neural firing (Snyder et al. 2000) and ITD sensitivity (Smith and Delgutte 2008) in response to high-pulse rate carriers. For this reason, we might have obtained higher firing rates with high-rate periodic stimuli had we modulated them as Laback and Majdak (2008) did. However, it is difficult to predict how this difference might impact the jitter effect.

Mechanism depends on short interpulse intervals. Sparse, preferred firing times characterized the ongoing responses evoked by high-rate jittered pulse trains (Figs. 2, 5, and 8). These preferred times were highly reproducible across stimulus repetitions for an individual neuron and were remarkably similar across neurons (Fig. 9), suggesting that jitter restores ongoing firing by a relatively low-level, deterministic mechanism. The spike-triggered averaging analysis shown in Fig. 12 demonstrates that neural spikes were triggered specifically by short interpulse intervals. The preferred firing times were accurately predicted by the occurrence of the very shortest intervals (Figs. 12 and 13). As such, the underlying mechanism must be highly nonlinear. We were unable to predict neural firing times using more conventional models such as linear filtering of the pulse train followed by thresholding ("linear-nonlinear model").

The behavior we observe, with respect both to pulse rate limits and the dependence on short interpulse intervals, is consistent with the physiology of low-voltage-activated K^+ currents ($I_{K,LVA}$) present in neurons at multiple levels of the auditory system, including the auditory nerve (Mo et al. 2002; Mo and Davis 1997), bushy and octopus cells in the ventral cochlear nucleus (Bal and Oertel 2001; Manis and Marx 1991; Rothman and Manis 2003), the medial superior olive (MSO) (Scott et al. 2005; Smith 1995; Svirskis et al. 2002), and perhaps to some extent in the IC (Sivaramakrishnan and Oliver 2001). Neurons expressing $I_{K,LVA}$ exhibit phasic responses to depolarizing current steps in vitro: activation of $I_{K,LVA}$ shortly after the stimulus onset increases membrane conductance and thereby increases the current required to reach spiking threshold (Manis and Marx 1991). Summated excitatory postsynaptic potentials evoked by periodic, high-rate intracochlear electrical stimulation may function in a similar manner, producing an

onset spike followed by a rapid increase in spiking threshold (Colburn et al. 2009).

The presence of $I_{K,LVA}$ renders neural spiking particularly sensitive to the rate of rise of the membrane potential (McGinley and Oertel 2006), because spike threshold must be reached within a short time window before $I_{K,LVA}$ dynamics produce a compensatory increase in membrane conductance. In this context, the short interpulse intervals in jittered pulse trains may elicit spikes because their effects summate temporally to produce sufficiently rapid increases in membrane potential.

Spike-triggered averaging in MSO neurons stimulated with intracellular noise currents in vitro show that in the subthreshold state, MSO neurons are triggered by rapid increases in current (Svirskis et al. 2002). In addition, these rapid increases are preceded by slower decreases in current, which allow membrane channels, including $I_{K,LVA}$, to partially deactivate, enhancing the response to the subsequent rapid rise (Svirskis et al. 2004). Interestingly, our spike-triggered averages also show a modest decrease in instantaneous pulse rate immediately preceding the rapid increase in pulse rate that triggers the spike (Fig. 12*A*).

In summary, among the snappy (jitter-sensitive) neurons, the dynamics of $I_{K,LVA}$ appear suitable to account for the adapted responses to high-rate periodic pulse trains and the sparse, preferred firing times evoked by the short interpulse intervals contained in high-rate jittered pulse trains. Given the convergence of ascending projections to the IC, the effects we measure may represent the effect of $I_{K,LVA}$ combined across multiple stages in the auditory brain stem. Because $I_{K,LVA}$ is present in cochlear nucleus neurons, we expect that pulse train jitter also affects IC responses to monaural stimulation.

It is possible that such channel dynamics are modulated by other factors. For example, the occurrence of two pulses in rapid succession after a long interpulse interval with jittered stimuli might result in greater spread of excitation along the tonotopic axis and therefore increased likelihood of firing. We further speculate that the more restrictive pulse rate limits and diminished jitter sensitivity in the sluggish neurons are due to other mechanisms, such as delayed inhibition (Nelson and Carney 2004; Smith and Delgutte 2008). Possibly, gradations in the contributions of inhibition, $I_{K,LVA}$, and other mechanisms underlie the continuum of sensitivities to pulse rate and jitter suggested by the clustering analysis (Fig. 3). Detailed computational modeling is needed to quantify the extent to which different mechanisms account for the observed physiology.

Comparison with other physiological studies. Using CI stimulation, Kirby and Middlebrooks (2010, 2012) measured gap detection thresholds at 254, 1,017, and 4,096 pps in the guinea pig auditory cortex. On average, gaps much greater than twice the mean interpulse intervals (i.e., equivalent to >100% jitter) were required to evoke spikes to the pulse after the gap, even in an unanesthetized preparation. This is consistent with our conclusion that the long intervals in the jittered pulse trains cannot account for restoration of ongoing firing, because our longest interpulse intervals were always less than twice the mean.

Studies in normal-hearing animals have compared neural responses to periodic and aperiodic pulsatile stimulation. Burkard and Palmer (1997) stimulated guinea pig VCN chopper neurons using periodic click trains and trains of maximum length sequences with interpulse intervals as short as 0.5 ms. There were no differences in mean firing rates, consistent with the absence of $I_{K,LVA}$ channels in chopper neurons and the hypothesized role of such channels in mediating the jitter effect. In the awake marmoset auditory cortex, Bendor and Wang (2007) showed that 50% jitter had little effect on firing rate responses of nonpitch-sensitive neurons to trains of Gaussian tone pips for pulse rates up to ~50 Hz, consistent with the present IC responses, where at least 70% jitter was necessary to have a substantial effect (Fig. 8). Pitch-sensitive cortical neurons, however, showed monotonically decreasing firing rates with increasing jitter for pulse rates as high as ~500 Hz, which was interpreted as a cortical specialization for encoding periodicity (Bendor and Wang 2010). It will be interesting to test the behavior of these neurons with CI stimulation.

Relation to "restarting" from binaural adaptation. Onset cues dominate the lateralization of high-rate pulsatile stimuli in normal hearing, a phenomenon referred to as "binaural adaptation" (Buell and Hafter 1988). Insertion of a single long or short interpulse interval can trigger a "restart" from adaptation, in that the pulse after the oddball interval has greater influence on lateralization than the preceding and subsequent pulses (Hafter and Buell 1990). Hypothesizing that degraded ITD discrimination at high pulse rates with CI is a manifestation of binaural adaptation, Laback and Majdak (2008) predicted that pulse train jitter would provide robust ITD sensitivity by continuously resetting the adaptation.

A point of debate is the extent to which long and short interpulse intervals mediate the jitter effect. Van Hoesel (2008a) argued that, because ITD discrimination with CI improves with decreasing pulse rate, the effect of jitter may result simply from transient reductions in instantaneous pulse rate (i.e., long interpulse intervals) and hence is not necessarily a consequence of resetting binaural adaptation. In support of this idea, van Hoesel (2008b) subsequently showed that insertion of a single short interval into a periodic 300-pps pulse train was insufficient to restart ITD sensitivity in bilateral CI subjects. In contrast, Goupell et al. (2009) used high-frequency filtered click trains to simulate CI stimulation in normal hearing listeners and found that ITD discrimination was better for 1,200-pps jittered stimuli than for 600-pps periodic stimuli. They argued that reduction of instantaneous pulse rate cannot account for this result because the longest interpulse interval in the jittered stimulus was shorter than the mean interpulse interval in the periodic stimulus.

Also in normal-hearing listeners, Brown and Stecker (2011) demonstrated that jittering a 400-pps train of high-frequency Gaussian tone pips increased the contribution of ongoing pulses to ITD discrimination relative to the leading pulse. Both the longest and shortest interpulse intervals contributed to lateralization, although there was a small tendency for the longest interval to have greater influence.

Our physiological results are most consistent with the interpretation of Goupell et al. (2009). On average, neural ITD sensitivity is far better for 640-pps jittered pulse trains than for 320-pps periodic stimuli (Fig. 7*D*). Moreover, we explicitly showed that short interpulse intervals are responsible for triggering spikes in adapted IC neurons (Fig. 12). Our results suggest that, physiologically, jitter does not produce a true restart from adaptation, at least at the level of the IC. Rather, it appears that IC neurons persist in an adapted state, but short interpulse intervals cause the membrane potential to transiently

exceed the adapted threshold. While the physiological results from the IC clearly favor short interpulse intervals as a trigger for the jitter effect, the term "binaural adaptation" may encompass several different mechanisms operating at different levels of the auditory system, and these various mechanisms may be affected differently by jitter.

Implications. In principle, ITD coding with bilateral CIs could be improved by using jittered pulse trains as carriers in a continuous interleaved sampling strategy (Laback and Majdak 2008). However, jitter may also degrade the representation of other sound properties. Most importantly, distortion of speech envelopes may outweigh the benefit to speech perception of restoring binaural unmasking. The present results, however, suggest an alternative scheme. Because it is specifically the short intervals that restore neural firing, it does not seem necessary to jitter the entire carrier pulse train. One could instead just insert short interpulse intervals at strategically selected times. For instance, using a 1,000-pps carrier, one might insert a 200-μs interpulse interval at the onset of every voice pitch period. This would presumably restore ongoing firing in the otherwise adapted ITD-sensitive neurons. By also imposing an ITD on these short interpulse intervals, ITD coding could be enhanced. Such a strategy may prove complementary to recent algorithms that lower the carrier pulse rate and lock stimulus pulses to specific waveform events to restore ITD coding without degrading speech intelligibility (Smith 2010).

Conclusions. We have shown that pulse train jitter reveals latent neural ITD sensitivity by restoring ongoing firing at high pulse rates. Neural spiking is triggered specifically by the shortest interpulse intervals. The results are qualitatively consistent with the effect of jitter on ITD perception of human CI users.

ACKNOWLEDGMENTS

The authors are grateful to Dr. David Ryugo for providing deaf white cats from his colony. The authors thank Connie Miller for expert surgical assistance and Melissa Wood for histological processing. The authors also give special thanks to Dr. Mitchell Day for suggesting the vector concatenation step of the clustering procedure.

GRANTS

This work was supported by National Institute on Deafness and Other Communication Disorders Grants R01-DC-005775 and P30-DC-005209.

DISCLOSURES

No conflicts of interest, financial or otherwise, are declared by the author(s).

AUTHOR CONTRIBUTIONS

Author contributions: K.E.H. and B.D. conception and design of research; K.E.H., Y.C., and B.D. performed experiments; K.E.H. and Y.C. analyzed data; K.E.H., Y.C., and B.D. interpreted results of experiments; K.E.H. prepared figures; K.E.H. drafted manuscript; K.E.H. and B.D. edited and revised manuscript; K.E.H., Y.C., and B.D. approved final version of manuscript.

REFERENCES

Aronoff JM, Yoon YS, Freed DJ, Vermiglio AJ, Pal I, Soli SD. The use of interaural time and level difference cues by bilateral cochlear implant users. *J Acoust Soc Am* 127: EL87–EL92, 2010.

Bal R, Oertel D. Potassium currents in octopus cells of the mammalian cochlear nucleus. *J Neurophysiol* 86: 2299–2311, 2001.

Bendor D, Wang X. Differential neural coding of acoustic flutter within primate auditory cortex. *Nat Neurosci* 10: 763–771, 2007.

Bendor D, Wang X. Neural coding of periodicity in marmoset auditory cortex. *J Neurophysiol* 103: 1809–1822, 2010.

Bronkhorst AW, Plomp R. Effect of multiple speechlike maskers on binaural speech recognition in normal and impaired hearing. *J Acoust Soc Am* 92: 3132–3139, 1992.

Brown AD, Stecker GC. Temporal weighting functions for interaural time and level differences. II. The effect of binaurally synchronous temporal jitter. *J Acoust Soc Am* 129: 293–300, 2011.

Buell TN, Hafter ER. Discrimination of interaural differences of time in the envelopes of high-frequency signals: integration times. *J Acoust Soc Am* 84: 2063–2066, 1988.

Burkard R, Palmer AR. Responses of chopper units in the ventral cochlear nucleus of the anaesthetised guinea pig to clicks-in-noise and click trains. *Hear Res* 110: 234–250, 1997.

Chung Y, Hancock KE, Nam S, Delgutte B. The upper limit of temporal coding of electric pulse trains in the inferior colliculus of awake animals wearing cochlear implants. *Abstr Assoc Res Otolaryngol* 35: 279, 2012.

Colburn HS, Chung Y, Zhou Y, Brughera A. Models of brainstem responses to bilateral electrical stimulation. *J Assoc Res Otolaryngol* 10: 91–110, 2009.

Devore S, Delgutte B. Effects of reverberation on the directional sensitivity of auditory neurons across the tonotopic axis: influences of interaural time and level differences. *J Neurosci* 30: 7826–7837, 2010.

Goupell M, Hancock K, Majdak P, Laback B, Delgutte B. Binaurally-coherent jitter improves neural and perceptual ITD sensitivity in normal and electric hearing. In: *The Neurophysiological Bases of Auditory Perception*, edited by Lopez-Poveda EA, Palmer AR, Meddis R. New York: Springer, 2010, p. 303–313.

Goupell MJ, Laback B, Majdak P. Enhancing sensitivity to interaural time differences at high modulation rates by introducing temporal jitter. *J Acoust Soc Am* 126: 2511–2521, 2009.

Hafter ER, Buell TN. Restarting the adapted binaural system. *J Acoust Soc Am* 88: 806–812, 1990.

Hancock KE, Noel V, Ryugo DK, Delgutte B. Neural coding of interaural time differences with bilateral cochlear implants: effects of congenital deafness. *J Neurosci* 30: 14068–14079, 2010.

Joris PX. Interaural time sensitivity dominated by cochlea-induced envelope patterns. *J Neurosci* 23: 6345–6350, 2003.

Kirby AE, Middlebrooks JC. Auditory temporal acuity probed with cochlear implant stimulation and cortical recording. *J Neurophysiol* 103: 531–542, 2010.

Kirby AE, Middlebrooks JC. Unanesthetized auditory cortex exhibits multiple codes for gaps in cochlear implant pulse trains. *J Assoc Res Otolaryngol* 13: 67–80, 2012.

Kuwada S, Batra R, Stanford TR. Monaural and binaural response properties of neurons in the inferior colliculus of the rabbit: effects of sodium pentobarbital. *J Neurophysiol* 61: 269–282, 1989.

Kuwada S, Yin TC, Syka J, Buunen TJ, Wickesberg RE. Binaural interaction in low-frequency neurons in inferior colliculus of the cat. IV. Comparison of monaural and binaural response properties. *J Neurophysiol* 51: 1306–1325, 1984.

Laback B, Majdak P. Binaural jitter improves interaural time-difference sensitivity of cochlear implantees at high pulse rates. *Proc Natl Acad Sci USA* 105: 814–817, 2008.

Laback B, Majdak P, Baumgartner WD. Lateralization discrimination of interaural time delays in four-pulse sequences in electric and acoustic hearing. *J Acoust Soc Am* 121: 2182–2191, 2007.

Litovsky R, Parkinson A, Arcaroli J, Sammeth C. Simultaneous bilateral cochlear implantation in adults: a multicenter clinical study. *Ear Hear* 27: 714–731, 2006.

Litvak L, Delgutte B, Eddington D. Auditory nerve fiber responses to electric stimulation: modulated and unmodulated pulse trains. *J Acoust Soc Am* 110: 368–379, 2001.

Loftus WC, Bishop DC, Oliver DL. Differential patterns of inputs create functional zones in central nucleus of inferior colliculus. *J Neurosci* 30: 13396–13408, 2010.

Manis PB, Marx SO. Outward currents in isolated ventral cochlear nucleus neurons. *J Neurosci* 11: 2865–2880, 1991.

McGinley MJ, Oertel D. Rate thresholds determine the precision of temporal integration in principal cells of the ventral cochlear nucleus. *Hear Res* 216–217: 52–63, 2006.

Middlebrooks JC, Snyder RL. Selective electrical stimulation of the auditory nerve activates a pathway specialized for high temporal acuity. *J Neurosci* 30: 1937–1946, 2010.

Mo ZL, Adamson CL, Davis RL. Dendrotoxin-sensitive K^+ currents contribute to accommodation in murine spiral ganglion neurons. *J Physiol* 542: 763–778, 2002.

Mo ZL, Davis RL. Endogenous firing patterns of murine spiral ganglion neurons. *J Neurophysiol* 77: 1294–1305, 1997.

Nelson PC, Carney LH. A phenomenological model of peripheral and central neural responses to amplitude-modulated tones. *J Acoust Soc Am* 116: 2173–2186, 2004.

Peissig J, Kollmeier B. Directivity of binaural noise reduction in spatial multiple noise-source arrangements for normal and impaired listeners. *J Acoust Soc Am* 101: 1660–1670, 1997.

Poon BB, Eddington DK, Noel V, Colburn HS. Sensitivity to interaural time difference with bilateral cochlear implants: development over time and effect of interaural electrode spacing. *J Acoust Soc Am* 126: 806–815, 2009.

Rothman JS, Manis PB. Differential expression of three distinct potassium currents in the ventral cochlear nucleus. *J Neurophysiol* 89: 3070–3082, 2003.

Ryugo DK, Cahill HB, Rose LS, Rosenbaum BT, Schroeder ME, Wright AL. Separate forms of pathology in the cochlea of congenitally deaf white cats. *Hear Res* 181: 73–84, 2003.

Ryugo DK, Rosenbaum BT, Kim PJ, Niparko JK, Saada AA. Single unit recordings in the auditory nerve of congenitally deaf white cats: morphological correlates in the cochlea and cochlear nucleus. *J Comp Neurol* 397: 532–548, 1998.

Schleich P, Nopp P, D'Haese P. Head shadow, squelch, and summation effects in bilateral users of the MED-EL COMBI 40/40+ cochlear implant. *Ear Hear* 25: 197–204, 2004.

Scott LL, Mathews PJ, Golding NL. Posthearing developmental refinement of temporal processing in principal neurons of the medial superior olive. *J Neurosci* 25: 7887–7895, 2005.

Seeber BU, Fastl H. Localization cues with bilateral cochlear implants. *J Acoust Soc Am* 123: 1030–1042, 2008.

Shepherd RK, Baxi JH, Hardie NA. Response of inferior colliculus neurons to electrical stimulation of the auditory nerve in neonatally deafened cats. *J Neurophysiol* 82: 1363–1380, 1999.

Sivaramakrishnan S, Oliver DL. Distinct K currents result in physiologically distinct cell types in the inferior colliculus of the rat. *J Neurosci* 21: 2861–2877, 2001.

Smith PH. Structural and functional differences distinguish principal from nonprincipal cells in the guinea pig MSO slice. *J Neurophysiol* 73: 1653–1667, 1995.

Smith ZM. Discrimination of interaural time differences in speech with an asynchronous cochlear implant sound coding strategy. *Assoc Res Otolaryngol Abs* 33: 128, 2010.

Smith ZM, Delgutte B. Sensitivity of inferior colliculus neurons to interaural time differences in the envelope versus the fine structure with bilateral cochlear implants. *J Neurophysiol* 99: 2390–2407, 2008.

Smith ZM, Delgutte B. Sensitivity to interaural time differences in the inferior colliculus with bilateral cochlear implants. *J Neurosci* 27: 6740–6750, 2007a.

Smith ZM, Delgutte B. Using evoked potentials to match interaural electrode pairs with bilateral cochlear implants. *J Assoc Res Otolaryngol* 8: 134–151, 2007b.

Snyder R, Leake P, Rebscher S, Beitel R. Temporal resolution of neurons in cat inferior colliculus to intracochlear electrical stimulation: effects of neonatal deafening and chronic stimulation. *J Neurophysiol* 73: 449–467, 1995.

Snyder RL, Vollmer M, Moore CM, Rebscher SJ, Leake PA, Beitel RE. Responses of inferior colliculus neurons to amplitude-modulated intracochlear electrical pulses in deaf cats. *J Neurophysiol* 84: 166–183, 2000.

Svirskis G, Kotak V, Sanes DH, Rinzel J. Enhancement of signal-to-noise ratio and phase locking for small inputs by a low-threshold outward current in auditory neurons. *J Neurosci* 22: 11019–11025, 2002.

Svirskis G, Kotak V, Sanes DH, Rinzel J. Sodium along with low-threshold potassium currents enhance coincidence detection of subthreshold noisy signals in MSO neurons. *J Neurophysiol* 91: 2465–2473, 2004.

van Hoesel RJ. Binaural jitter with cochlear implants, improved interaural time-delay sensitivity, and normal hearing. *Proc Natl Acad Sci USA* 105: E51, author reply E52, 2008a.

van Hoesel RJ. Contrasting benefits from contralateral implants and hearing aids in cochlear implant users. *Hear Res*; http://dx.doi.org/10.1016/j.heares.2011.11.014.

van Hoesel RJ. Exploring the benefits of bilateral cochlear implants. *Audiol Neurootol* 9: 234–246, 2004.

van Hoesel RJ. Observer weighting of level and timing cues in bilateral cochlear implant users. *J Acoust Soc Am* 124: 3861–3872, 2008b.

van Hoesel RJ, Tyler RS. Speech perception, localization, and lateralization with bilateral cochlear implants. *J Acoust Soc Am* 113: 1617–1630, 2003.

Vollmer M, Leake PA, Beitel RE, Rebscher SJ, Snyder RL. Degradation of temporal resolution in the auditory midbrain after prolonged deafness is reversed by electrical stimulation of the cochlea. *J Neurophysiol* 93: 3339–3355, 2005.

Xu SA, Shepherd RK, Chen Y, Clark GM. Profound hearing loss in the cat following the single co-administration of kanamycin and ethacrynic acid. *Hear Res* 70: 205–215, 1993.

Zurek PM. Binaural advantages and directional effects in speech intelligibility. In: *Acoustical Factors Affecting Hearing Aid Performance*, edited by Studebaker GA, Hochberg I. Boston, MA: Allyn and Bacon, 1992.